20. PHYSICAL PROPERTIES OF SEDIMENTS FROM THE GALAPAGOS REGION AND THEIR IMPLICATIONS FOR HYDROTHERMAL CIRCULATION[1]

Shun-ichiro Karato,[2] Ocean Research Institute, University of Tokyo, Nakano Tokyo 164, Japan
and
Keir Becker, Scripps Institution of Oceanography, University of California, San Diego, La Jolla, California

ABSTRACT

Detailed measurements of physical properties, including wet-bulk density, water content (porosity), sonic velocity, thermal conductivity, and shear strength were made for sediments from the Galapagos mounds area cored by the hydraulic piston corer.

Sediments in this area include manganese oxides, granular green clays, nongranular green clays (intermediate between granular green clays and pelagic sediments), and pelagic sediments. Average values of physical properties appear in Table 1.

The difference in sonic velocity and density between hydrothermal materials and pelagic sediments may be responsible for the complex seismic reflection pattern at mound sites. However, the depth variation of acoustic impedance in holes which are not at mound sites is smooth, and there are no obvious contrasts to account for regional seismic reflectors at 7 and 15 meters depth.

The depth gradients of porosity and therefore of density (and thermal conductivity) of pelagic sediments in the mounds area are very large and correlate well with surface heat flow. This suggests that the high depth gradients may be attributed to the effect of hydrothermal circulation and that hydrothermal convection cells may be essentially fixed with the moving plate.

Based on the porosity–depth relation found in this area, the hydraulic impedance of sediment layers is calculated as a function of their thickness, using the porosity–permeability relation of Bryant et al. (1974). The hydraulic impedance of the sediment layer increases with thickness and at several tens of meters thickness it becomes comparable to that of the basement rock layer, if the basement layer is 2 ~ 3 km thick and has an average permeability of 2 ~ 30 millidarcy.

INTRODUCTION

During Leg 70 of the Deep Sea Drilling Project (DSDP), undisturbed sediments were successfully sampled using the hydraulic piston corer. This enabled us to make detailed studies of their physical properties, which are fundamental to understanding the physical processes that occur in the oceanic crust.

Sediments were cored in 12 holes at 5 sites. These locations include various types of geothermal regimes which are considered to result primarily from hydrothermal circulation in the oceanic crust.

The circulation of seawater should affect the physical properties of the sediments; conversely it may be largely controlled by them, especially by the hydraulic properties of sediment layers.

Therefore, it is interesting to explore those interrelationships between the physical properties of the sediments and the circulation of seawater that may be inferred from heat flow and geochemical measurements.

In this paper, we will first summarize the physical properties of sediments and examine the relations among them. Next we will discuss the spatial variation of these properties and implications for the nature of hydrothermal circulation. Finally, the hydraulic properties of the sediment layer will be examined, and their implications for hydrothermal circulation discussed.

PHYSICAL PROPERTIES OF SEDIMENTS

Several kinds of sediments, including pelagic sediments, green clays, and manganese oxides, were found in the Galapagos mounds area. While on board the *Glomar Challenger*, we measured the wet-bulk density, water content, sonic velocity, thermal conductivity, and shear strength of samples taken at approximately 1- to 2-meter intervals for each core. Porosity and grain density were calculated from wet-bulk density and water content.

The wet-bulk density of sediments was measured by GRAPE (Gamma Ray Attenuation Porosity Evaluator) and gravimetric measurement procedures following Boyce (1976). Gravimetric measurements of water content and porosity were made by weighing wet and dry (heated at 110°C for 24 hr.) samples using a triple beam balance. Wet-bulk densities measured by the two methods agree within the error range of a few percent.

Sonic velocity was measured using the Hamilton Frame velocimeter (Boyce, 1976). Reliability of measurements was checked by repeated measurement of standards and was shown to be about 1%. The correction of liner thickness (D_L) and delay time (T_L) was made using the average value of $D_L = 0.256$ cm and $T_L = 1.180$ μs respectively.

Thermal conductivity measurements were made by the needle probe method (Von Herzen and Maxwell, 1959). Instrumentation problems limited absolute accuracy of laboratory values to about 5% (see Becker et al., this volume), but relative variations of conductivity were much more accurately determined.

[1] Honnorez, J., Von Herzen, R. P., et al., *Init. Repts. DSDP*, 70: Washington (U.S. Govt. Printing Office).

[2] Present address: Research School of Earth Sciences, The Australian National University, Canberra 2600, Australia.

Shear strength was measured using vane shear strength equipment, applying a torque on samples (Boyce, 1977).

All measurements were made at room temperatures and atmospheric pressure. No effort was made to convert laboratory data into *in situ* values, since the temperature and pressure effects on these physical properties are small and correction is well within the experimental error (e.g., Hamilton, 1976).

The distributions of physical properties for each site are shown in Figures 1 through 5. (Sediments from Site 510 were cored by drilling or punch-coring and showed evidences of large deformation in sampling processes. Therefore, the data for Site 510 are not reliable compared with those of other sites.) Means and standard deviations of measured values are given for the four sediment types in Table 1. Grain densities and (in general) other physical properties systematically covary among these types in the order in which they are listed—e.g., manganese oxides are more dense, have the highest velocities, and are least porous. An exception is the nongranular green clays, which are the most porous sediment and, as a result, have the lowest bulk densities and thermal conductivities.

In Figures 6 through 8, thermal conductivity, sonic velocity, and shear strength are plotted against wet-bulk density.

Figure 6 shows a good correlation between the wet-bulk density and thermal conductivity of pelagic sediments. For green clays, this relation is less clear, probably because of the variation of chemical composition in green clays. However, the thermal conductivity versus density trend of green clays is clearly different from that of pelagic sediments: At equal densities, green clays have lower thermal conductivities than do pelagic sediments. This suggests that green clays with zero porosity have lower thermal conductivity than do calcite or quartz.

Figure 7 illustrates a velocity versus density relation. In contrast to thermal conductivity, sonic velocity of pelagic sediments is relatively insensitive to density in the range observed in this area. This observation is compatible with the velocity versus density relation proposed by

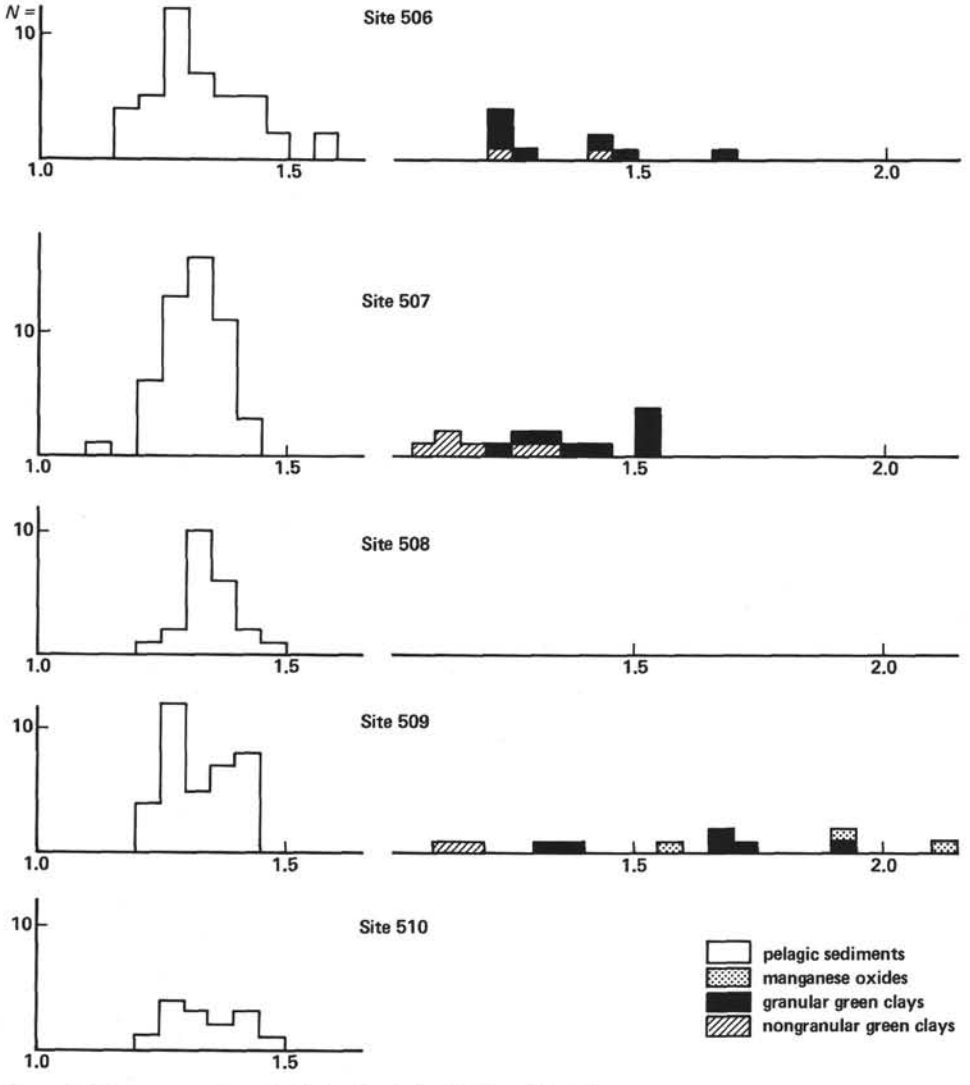

Figure 1. Histograms of wet-bulk density (g/cm^3), Sites 506–510.

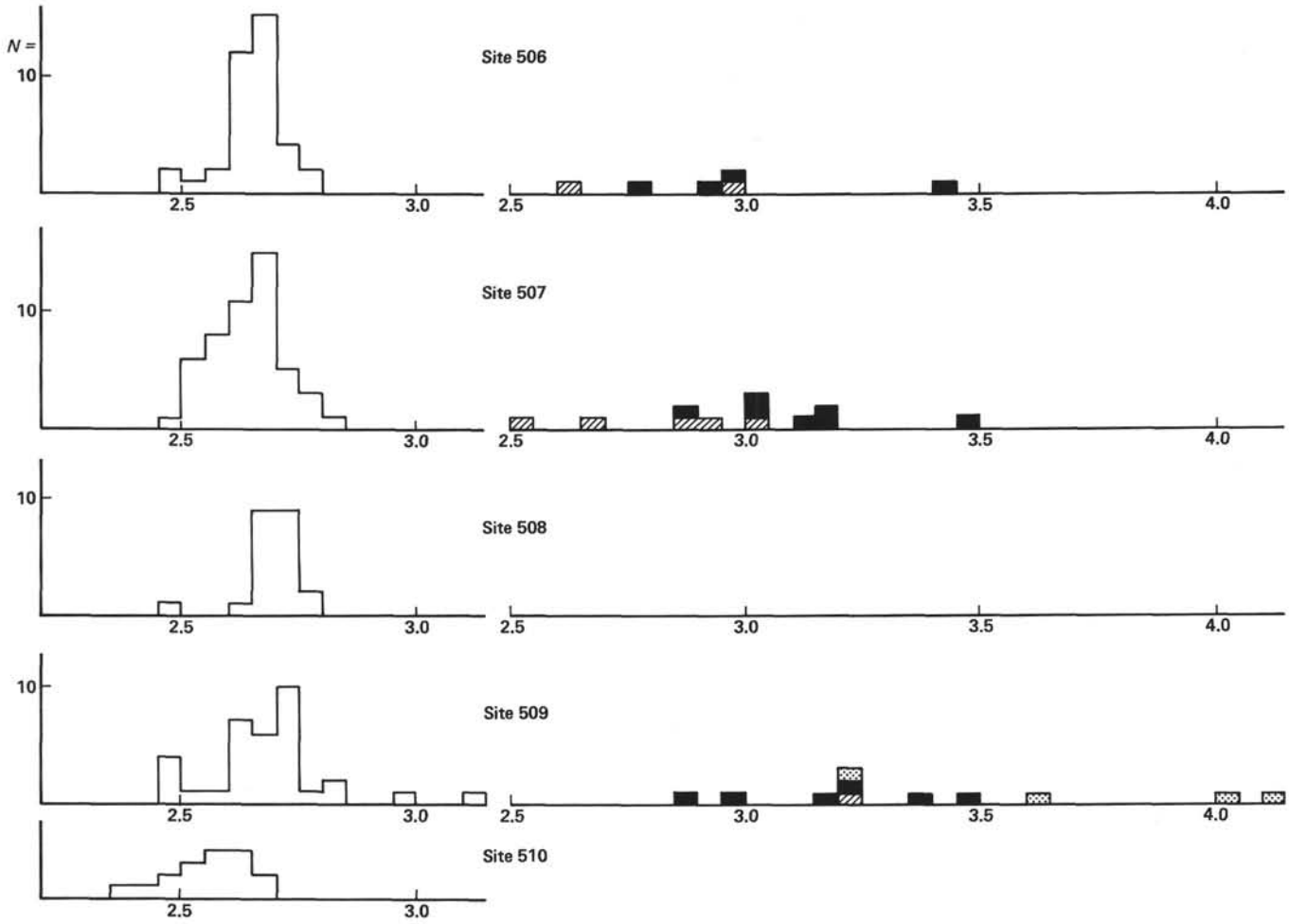

Figure 2. Histograms of grain density (g/cm^3), Sites 506–510. (See key to Fig. 1.)

Nafe and Drake (1957). The theoretical curves of Nafe and Drake's relation ($N = 4,5$) for calcareous sediments are also plotted for comparison. The high velocity of manganese oxides and green clays is shown to result mainly from their high density.

Shear strength versus density is shown in Figure 8. Good correlation is observed for pelagic sediments and for nongranular green clays: The larger the density, the larger the shear strength. Such a trend cannot be observed for granular green clays, probably because of the effect of granular texture. When granular texture develops, shear strength may decrease because the cohesion between grains is weak. The slight trend of decreasing shear strength of granular green clay with increasing density could be explained by the development of granular texture with increasing density.

DEPTH VARIATION OF PHYSICAL PROPERTIES

The depth variation of wet-bulk density, porosity, sonic velocity, acoustic impedance, and thermal conductivity for all holes is shown in Figures 9 through 13.

In those holes where both pelagic and hydrothermal sediments were cored (Holes 506, 506C, 506D, 507D, 509B), physical properties vary irregularly with depth. The irregular variation of acoustic impedance in these holes is consistent with the complex seismic reflection pattern observed at mounds (Lonsdale, 1977). In contrast, the properties of pelagic sediments, whether or not interbedded with hydrothermal materials, vary smoothly with depth. There are no obvious contrasts to account for regional seismic reflectors at 7 and 15 meters depth (Lonsdale, 1977). Therefore, we prefer to attribute these reflectors to interference patterns similar to those seen in other equatorial Pacific carbonates (Mayer, 1979), rather than to previously postulated ash layers (Lonsdale, 1977) or regional hydrothermal layers (Natland et al., 1979).

The depth variations of the physical properties of pelagic sediments are summarized in Table 2, where the results of linear regression for physical properties versus depth are given. It should be noted that in the thin sediment cover at Sites 506 to 509, the depth gradient of porosity is very high, -0.2 to -0.6%/m, compared to thicker pelagic sections (about -0.05 to -0.1%/m; e.g., Hamilton, 1976). In Hole 510, with 110 meters of sediment thickness, gradients in physical properties are "normal" in the upper section, but near basement (i.e., within 30 m) become higher and comparable to those of Sites 506 to 509. Such near-basement high-depth gradients of physical properties are more clearly shown for

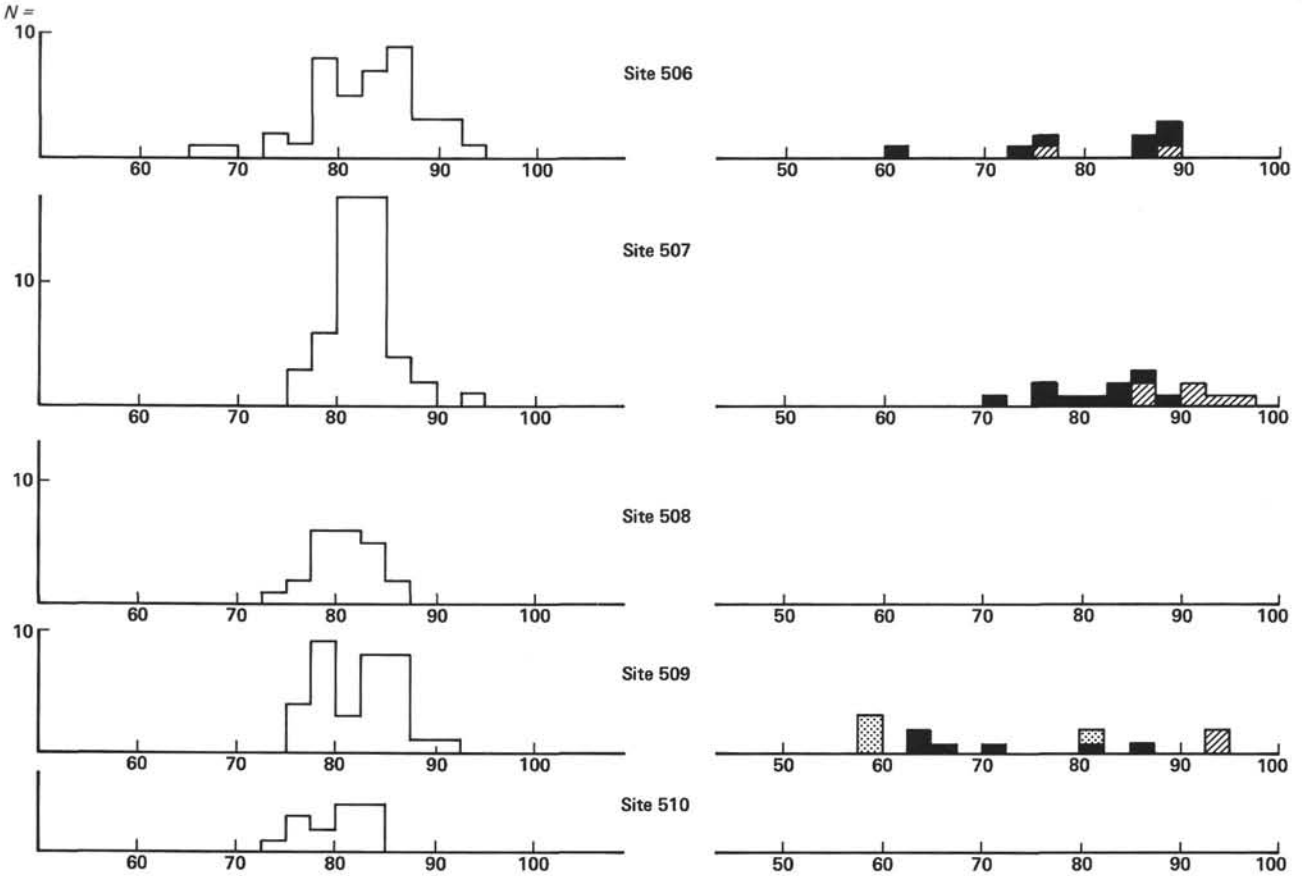

Figure 3. Histograms of porosity (%), Sites 506–510 (See key to Fig. 1.).

Sites 504 and 505 of Leg 69, where thick sediment sections (about 250 m) were cored by the hydraulic piston corer (Wilkens and Langseth, in press). This fact suggests that the high-depth gradient results from some sediment–basement interaction near the spreading center, as opposed to a more general physical process such as gravity compaction.

In Figure 14, the depth gradients of porosity and density are plotted against surface heat flow (Becker et al., this volume).

The good correlation between depth gradients of physical properties and surface heat flow again suggests that the high-depth gradients may result from some kind of sediment–basement interaction; more specifically, we suggest that they arise from the transfer between basement and sediment of hydrothermal fluids and/or conducted and advected heat, all of which are intimately related to surface heat flow.

It is important to note in Figure 14 that the values of the depth gradients correlate with *present-day* surface heat flow. There may be two possible interpretations for this observation. One is to assume that the depth gradients were essentially established by a recent event. Another possibility is that hydrothermal cells may be fixed with respect to the moving plate, in which case depth gradients would have been caused by processes occurring throughout the crust's history.

The first interpretation may be less likely than the second for the following reasons. The most plausible possibility for a recent event may be a recent rapid formation of mounds (Becker et al., this volume). Therefore (were the first interpretation valid), high depth gradients would be found only where mounds are being or have been formed. However, the high depth gradients are found not only in the mounds area but also at Sites 504, 505, and 510, where there is no evidence for mounds formation. Further, it may be unrealistic to assume that the active hydrothermal circulation, which occurred in the sediment columns when they were located closer to the ridge crest, has not caused the high depth gradients in physical properties.

The arguments suggest that the high depth gradients were caused by processes occurring throughout the crustal history. This may in turn imply that the hydrothermal cells are fixed with respect to the moving plate. If not, sediment columns would have experienced both high and low heat-flow regimes in their history, and once the high gradients have been established in the high heat-flow regime it may be difficult to "erase" them, as suggested by the occurrence of near-basement high depth gradients of physical properties at Sites 504, 505, and 510.

It is interesting to compare these arguments with the experiments of Green (1980) on the temporal and spatial development of hydrothermal cells at the Galapagos Spreading Center; these indicate that, after 0.2 to 0.3 m.y. of spreading, the cellular hydrothermal system moves with the spreading plate. Thus, outside about 10

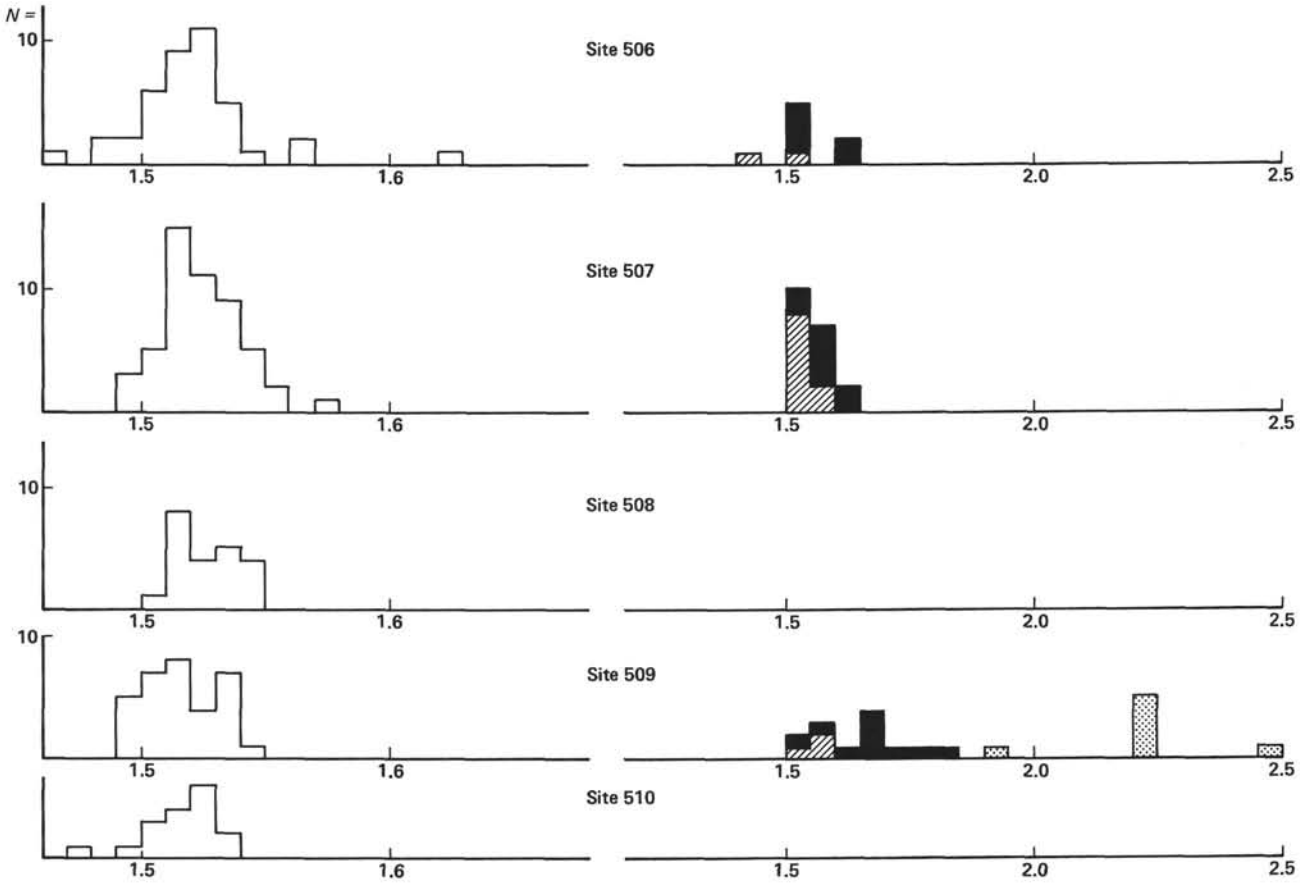

Figure 4. Histograms of sonic velocity (km/s), Sites 506–510. (See key to Fig. 1.) Note that the scale of velocity is different between pelagic and hydrothermal sediments.

km from the axis, where the first significant (~10 m) continuous sediment layer accumulates, the geothermal regime of a section of the spreading crust remains essentially the same (until the hydrothermal system damps out). This result is quite consistent with our arguments.

HYDRAULIC PROPERTIES OF SEDIMENT LAYERS

Bryant et al. (1974) has suggested a relation between porosity ϕ and permeability K_{sed} of oceanic sediments as

$$K_{sed} = 10^{-6} (\phi/(1 - \phi))^5 \text{ darcy}, \quad (1)$$

Since this relation holds for a wide range of porosity and for various kinds of sediments, it is reasonable to assume that it also holds for sediments in this area.

Assuming relationship (1) one can estimate the hydraulic impedance of sediment layer I by the following equation:

$$I = \int_0^h dz/K_{sed}(z) = 10^6 \text{ (darcy)}^{-1}\, x \int_0^h dz \left(\frac{1 - \phi(z)}{\phi(z)}\right)^5 \quad (2)$$

where h is the thickness of the sediment layer and z is depth, using the porosity versus depth relationship given previously.

In Figure 15, hydraulic impedance versus sediment-layer thickness relations are plotted for the various values of surface porosity ϕ_0 and $d\phi/dz$, which is defined by

$$\phi(z) = \phi_0 + (d\phi/dz)z \quad (3)$$

Since porosity decreases rapidly with depth, the permeability of sediments also decreases rapidly with depth: The permeability of sediments near the basements is about two orders of magnitude less than that of the surface. As a result, the hydraulic impedance of the sediment layer increases rapidly with increasing thickness, compared to a theoretically constant permeability layer.

When the hydraulic impedance of the sediment layer exceeds that of the basement layer, direct discharge and recharge of water through the sediments is inhibited, except at active faults or where topographically focused. As these local conduits are sealed off (by further sedimentation and/or hydrothermal precipitation), hydrothermal circulation is confined within the basement

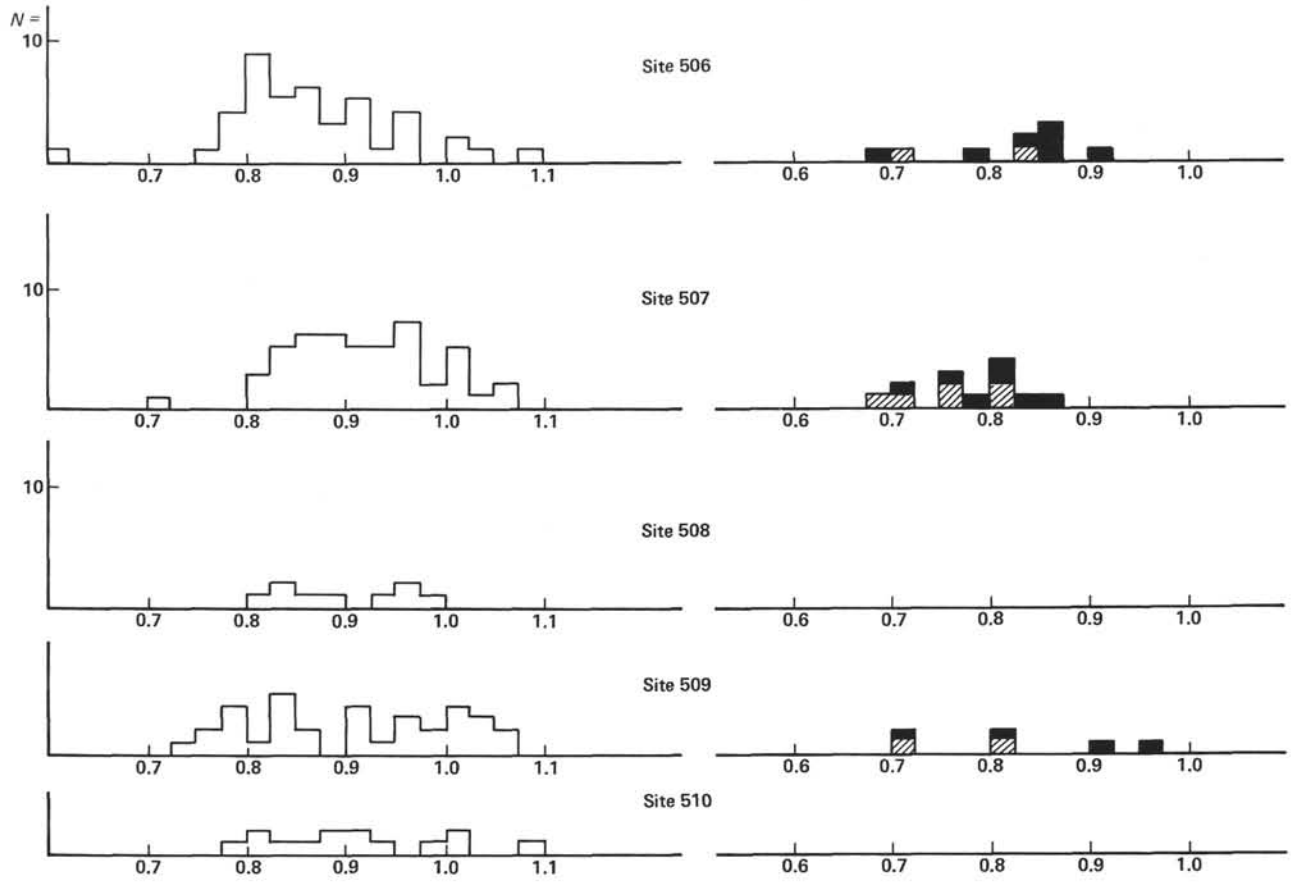

Figure 5. Histograms of thermal conductivity (W/mK), Sites 506–510. (See key to Fig. 1.)

Table 1. Average values of physical properties of sediments from Leg 70.

Sediment	Wet-Bulk Density (g/cm^3)	Grain Density (g/cm^3)	Porosity (%)	Sonic Velocity (km/s)	Thermal Conductivity (W/mK)	Shear Strength (g/cm^2)
Manganese oxides	1.98 ± 0.26 (N = 4)	3.75 ± 0.36 (N = 4)	64.0 ± 10.3 (N = 4)	2.22 ± 0.07 (N = 8)	—	—
Granular green clays	1.46 ± 0.19 (N = 22)	3.13 ± 0.23 (N = 17)	77.9 ± 8.5 (N = 22)	1.61 ± 0.09 (N = 26)	0.80 ± 0.07 (N = 18)	63 ± 34 (N = 18)
Nongranular green clays	1.20 ± 0.10 (N = 10)	2.74 ± 0.28 (N = 10)	89.8 ± 5.4 (N = 10)	1.55 ± 0.02 (N = 14)	0.78 ± 0.05 (N = 10)	78 ± 58 (N = 11)
Pelagic sediments	1.32 ± 0.09 (N = 161)	2.65 ± 0.08 (N = 161)	82.2 ± 4.2 (N = 161)	1.51 ± 0.02 (N = 158)	0.91 ± 0.08 (N = 147)	111 ± 61 (N = 141)

layer, where it may redistribute heat flow, but not change the regional mean heat flow. Therefore, the approach of the mean of observed values of heat flow to a theoretical prediction suggests that the bulk hydraulic impedance of the sediment layer has greatly exceeded that of the basement layer.

At the Galapagos Spreading Center, Anderson and Hobart (1976) place the regional transition zone to conductive heat flow at 4 to 6 m.y., where there is 200 to 300 meters of sediment. However, at the mounds area, mean observed heat flows first approach a theoretical value at about 1 m.y., with about 50 meters sediment cover. We suggest that at this thickness, the sediment's hydraulic impedance is comparable to that of the basement, so that generalized, diffuse fluid flow through the sediments is stopped. The discontinuity in the gradients

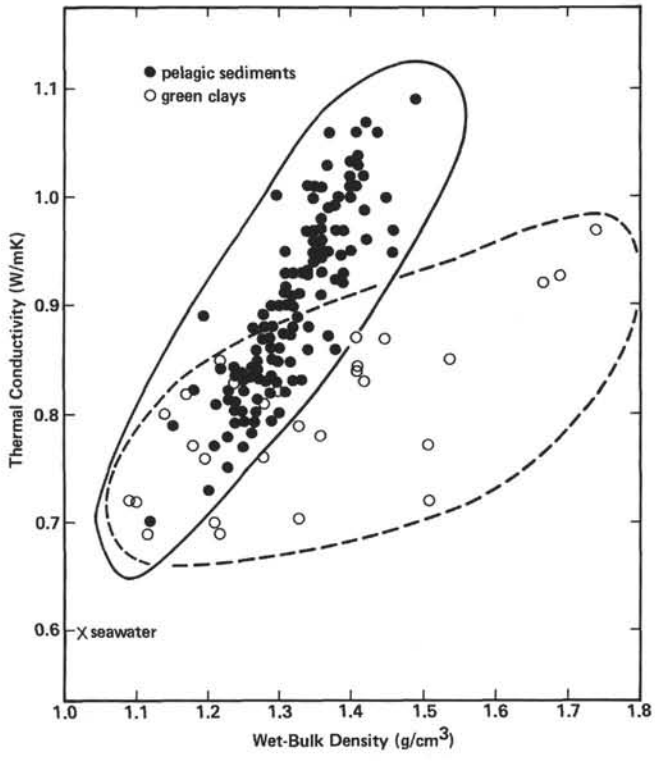

Figure 6. Thermal conductivity versus wet-bulk density.

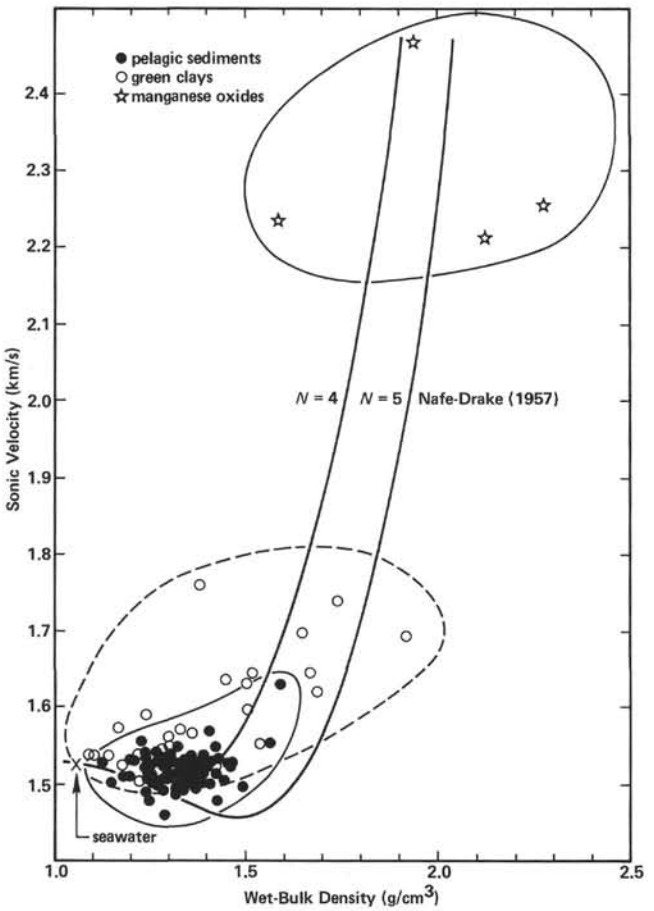

Figure 7. Sonic velocity versus wet-bulk density. (Curves are the theoretical relations by Nafe and Drake [1957] for parameters $N=4$ and 5.)

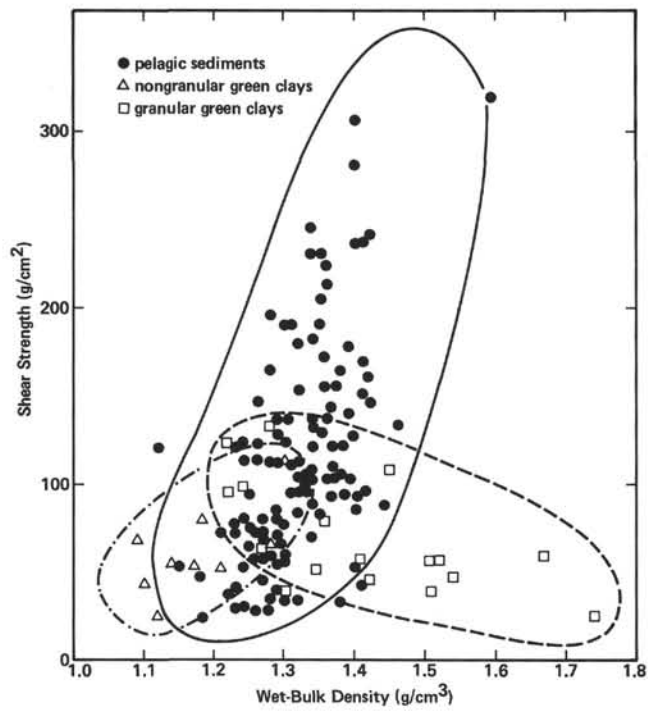

Figure 8. Shear strength versus wet-bulk density.

of physical properties at this sediment thickness may reflect the cessation of fluid flow through the sediments, if it can be shown that fluid flow processes are responsible for the high gradients in the near-basement sediment properties.

Assuming that the hydraulic impedance of 50 meters of sediment cover is comparable to that of the basement rock,

$$\int_0^{50} dz/K_{sed}(z) = 10^{17} - 10^{18}(\mathrm{m}^{-1}) = H/K_{base} \quad (4)$$

where H is the thickness of the basement layer where hydrothermal circulation occurs and K_{base} is the average permeability of the basement layer. From the observed heat flow pattern at the Galapagos Spreading Center, H is estimated at 2 to 3 km (Green, 1980). Then equation (4) gives

$$K_{base} = 2\text{–}30 \text{ (millidarcy)} \quad (5)$$

This value is in good agreement with the independent estimate of K_{base} by Anderson et al. (1977).

DISCUSSION AND CONCLUSIONS

Two important observations constrain our interpretation of the data on physical properties in terms of hydrothermal processes occurring within the young oceanic crust at the Galapagos Spreading Center (GSC). First, anomalously high gradients in the sediment's physical properties are associated with this hydrothermally active area, but are limited to the thin sediment cover of Sites 506 to 509 and to the lower sections of thicker sediment at Sites 504 and 505 of Leg 69 and 510 of this leg. Second, the values of these high gradients correlate well with surface heat flow. Since the surface heat flow is strongly perturbed by active hydrothermal circulation (Williams et al., 1974; Green et al., 1981), we propose a hydrothermal mechanism for the formation of the gradients in properties and interpret the discontinuity in the gradients at about 50 meters of sediment cover in terms of a major change in the nature of the hydrothermal systems.

The gradients in the sediments' physical properties all correlate with the high gradient in porosity. In the pelagic ooze at the Galapagos Spreading Center, porosity is very high (80–90%), mainly because of the shell structure of the ooze. The dissolution of these shells provides a mechanism for the reduction of porosity in the absence of significant overburden pressure. Such dissolution should occur more effectively with hydrothermal water percolating through the sediments. Since discharge of warm thermal fluids and recharge of cold bottom waters are often associated with high and low heat flows at our sites (Becker et al., this volume), a hydrothermal dissolution process (Bender, this volume; Borella et al., this volume) can explain both the regionally high gradients in physical properties as well as the local correlation of these gradient values with surface heat flow.

The return to normal gradients of physical properties in sediments more than about 50 meters above basement

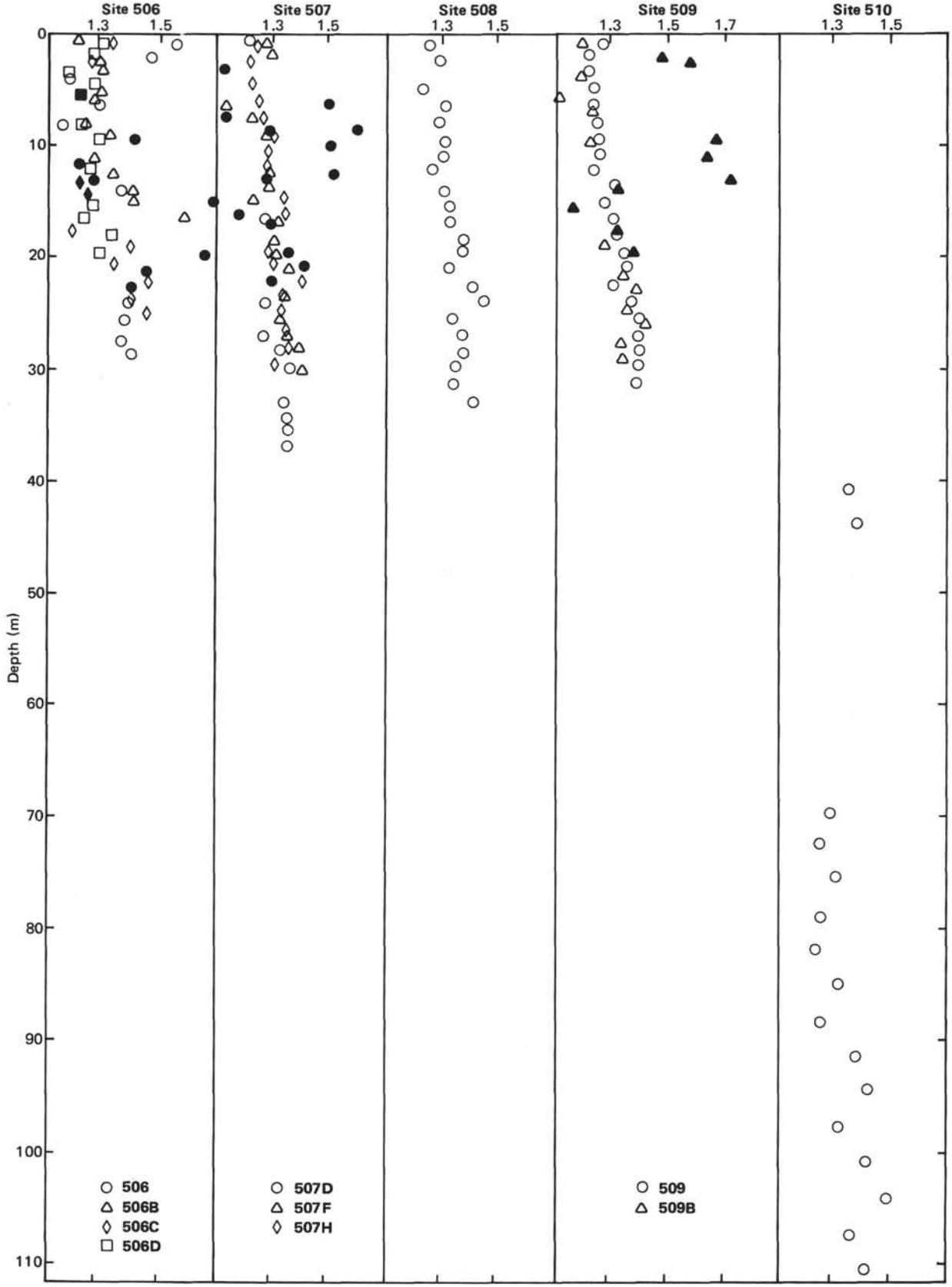

Figure 9. Depth variations of wet-bulk density (g/cm^3). (Open symbols = pelagic sediments, closed symbols = hydrothermal materials.)

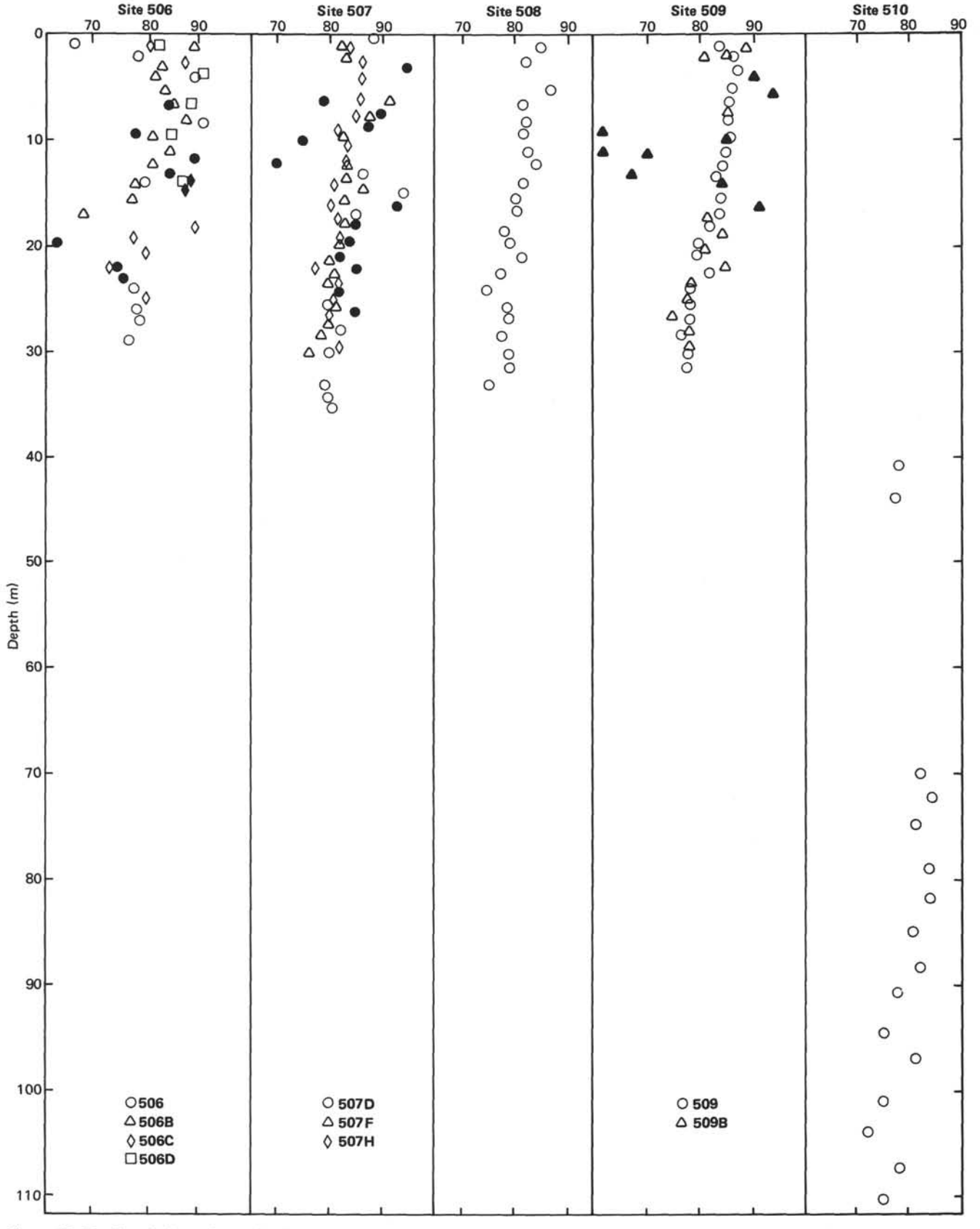

Figure 10. Depth variations of porosity (%). (Open symbols = pelagic sediments, closed symbols = hydrothermal materials.)

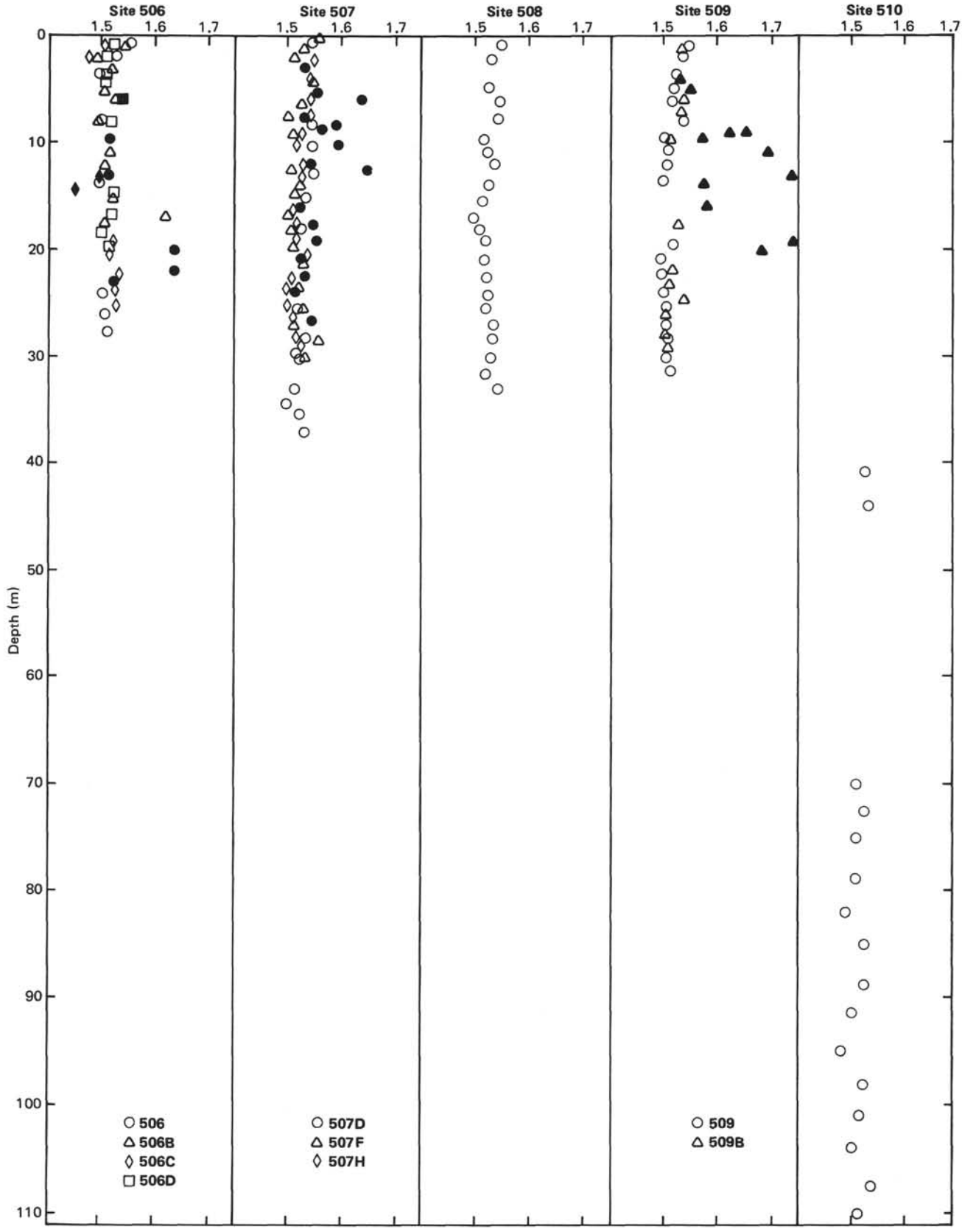

Figure 11. Depth variations of sonic velocity (km/s). (Open symbols = pelagic sediments, closed symbols = hydrothermal materials.)

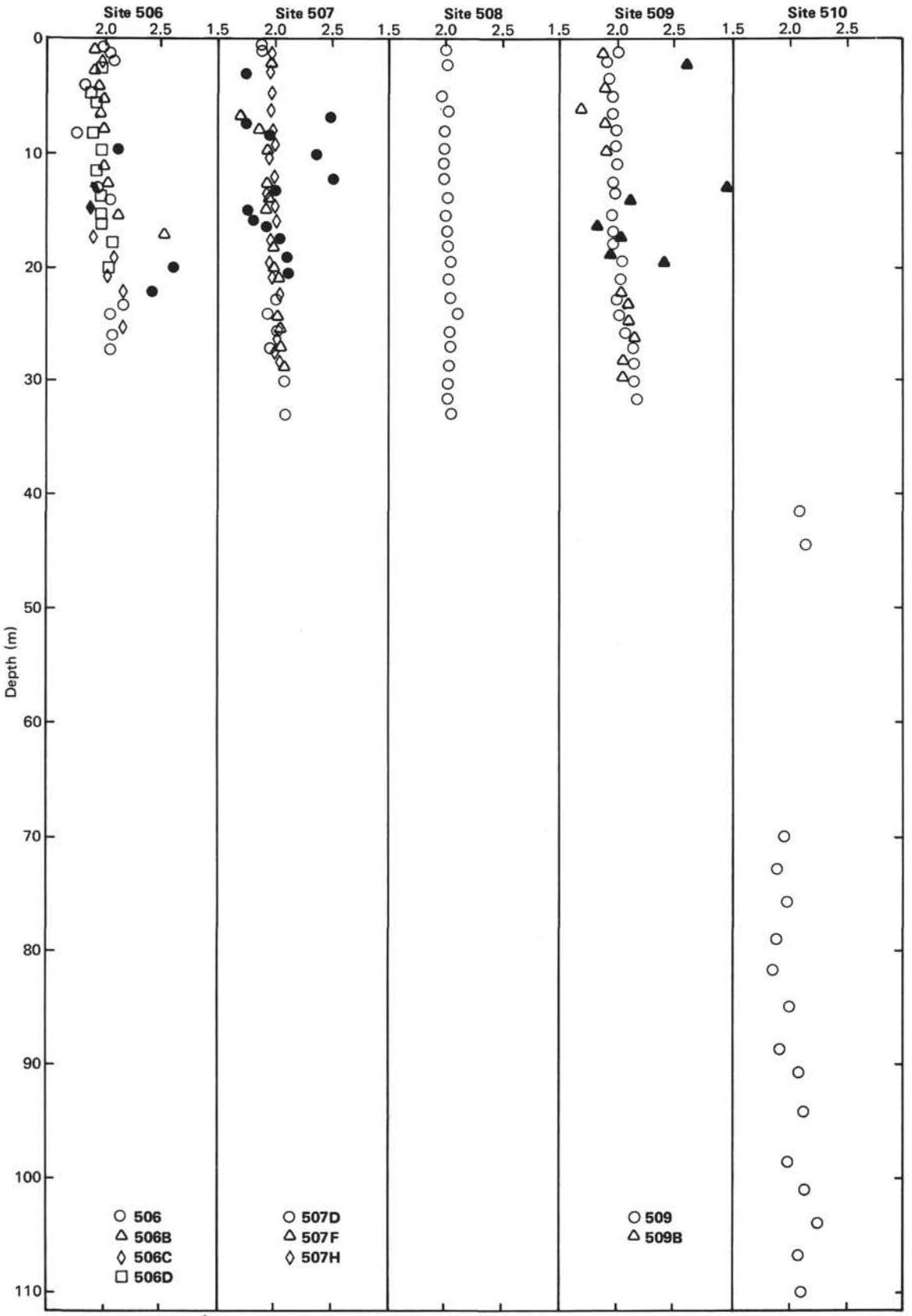

Figure 12. Depth variations of acoustic impedance ($\times 10^5$ g/s cm^2). (Open symbols = pelagic sediments, closed symbols = hydrothermal materials.)

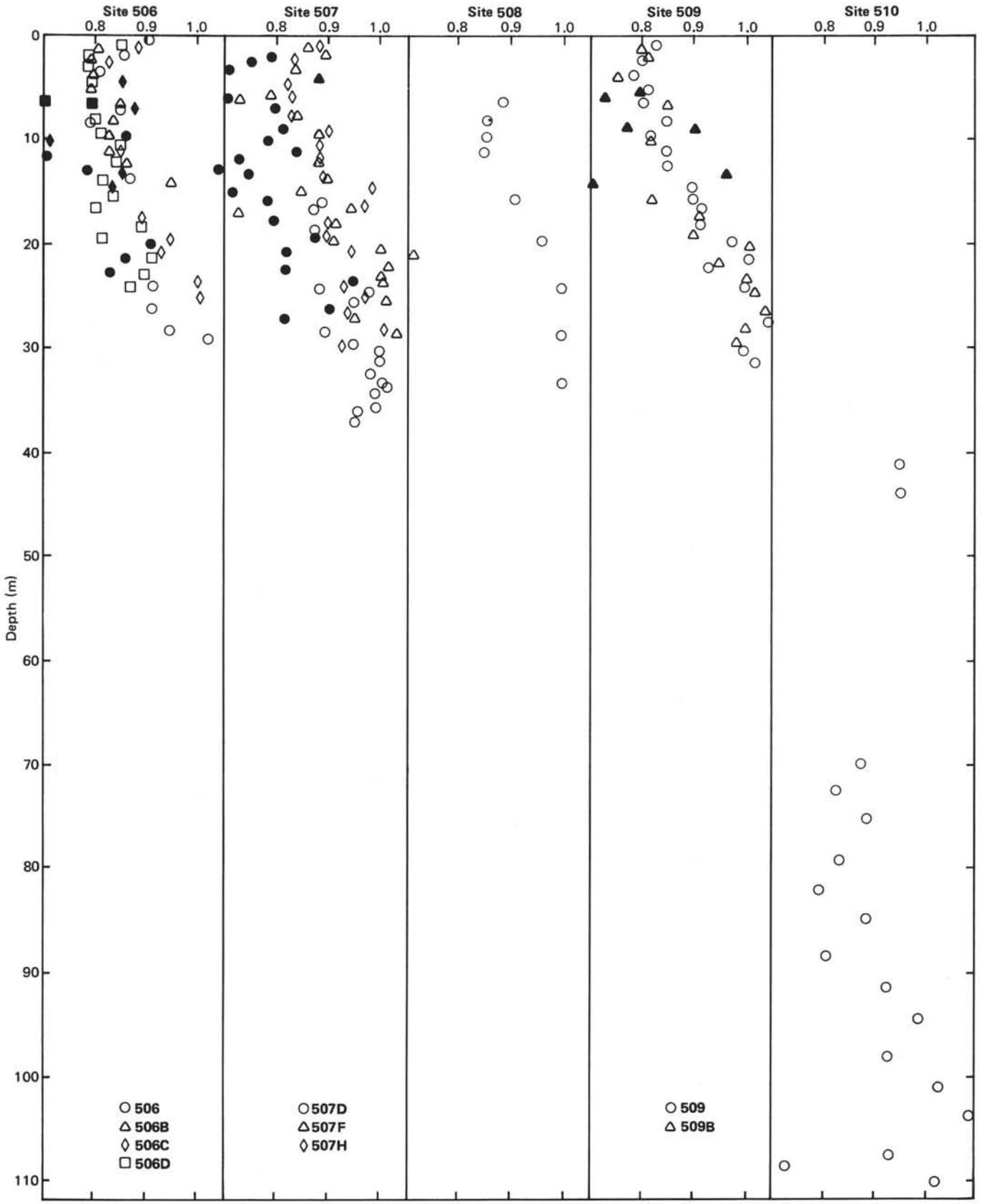

Figure 13. Depth variations of thermal conductivity (W/mK). (Open symbols = pelagic sediments, closed symbols = hydrothermal materials.)

Table 2. Results of linear regression for physical properties versus depth relations (z = sub-bottom depth in meters).

Hole	Density (g/cm^3)	Porosity (%)	Thermal Conductivity (W/mk)
506	1.32(±0.06) + 0.0080(±0.0020)z	91.3(±2.5) − 0.50(±0.13)z	0.762(±0.031) + 0.0073(±0.0015)z
506B	1.25(±0.03) + 0.0083(±0.0033)z	88.1(±1.5) − 0.60(±0.16)z	0.773(±0.020) + 0.0084(±0.0024)z
506C	1.27(±0.07) + 0.0053(±0.0035)z	85.8(±4.0) − 0.33(±0.21)z	0.837(±0.027) + 0.0057(±0.0015)z
506D	1.21(±0.03) + 0.0040(±0.0020)z	88.5(±1.8) − 0.22(±0.14)z	0.763(±0.019) + 0.0050(±0.0012)z
507D	1.25(±0.02) + 0.0030(±0.0010)z	88.4(±0.9) − 0.23(±0.03)z	0.749(±0.067) + 0.0062(±0.0023)z
507F	1.23(±0.02) + 0.0051(±0.0013)z	87.2(±1.6) − 0.30(±0.08)z	0.764(±0.030) + 0.0089(±0.0017)z
507H	1.24(±0.01) + 0.0042(±0.0008)z	85.6(±0.8) − 0.21(±0.05)z	0.832(±0.019) + 0.0053(±0.0011)z
508	1.27(±0.02) + 0.0041(±0.0008)z	84.8(±0.8) − 0.25(±0.04)z	0.786(±0.019) + 0.0062(±0.0010)z
509	1.22(±0.01) + 0.0064(±0.0005)z	87.9(±0.6) − 0.36(±0.03)z	0.742(±0.015) + 0.0099(±0.0008)z
509B	1.19(±0.02) + 0.0071(±0.0011)z	90.7(±1.5) − 0.48(±0.08)z	0.732(±0.025) + 0.010(±0.001)z
510			
(70–80 m)	1.43(±0.38) − 0.0021(±0.0052)z	83.3(±17.6) + 0.006(±0.236)z	0.998(±0.376) − 0.0020(±0.0051)z
(80–110 m)	1.27(±0.39) + 0.0055(±0.0022)(z-80)	82.7(±15.8) − 0.28(±0.09)(z-80)	0.810(±0.374) + 0.0074(±0.0021)(z-80)

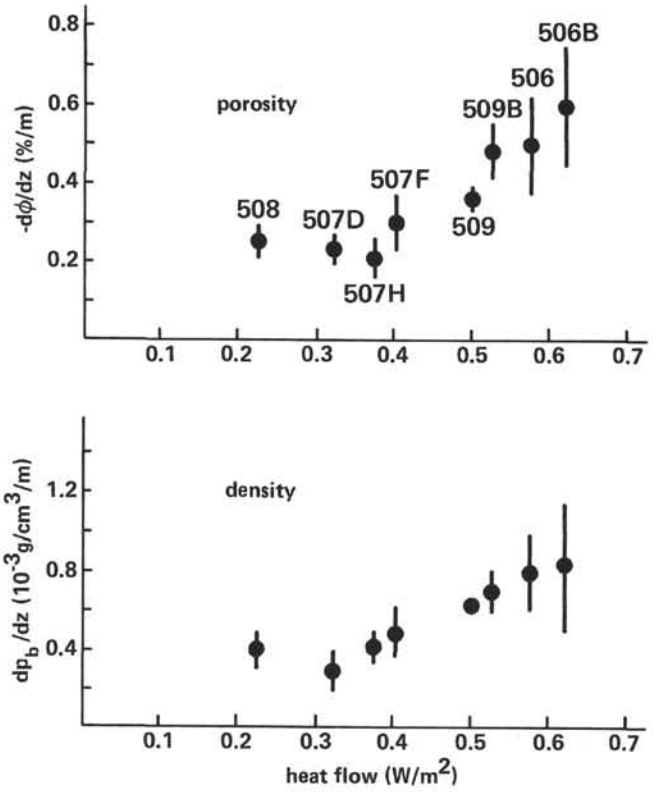

Figure 14. Depth gradients of wet-bulk density and porosity versus surface heat flow (Becker et al., this volume). (Vertical bars indicate standard deviation.)

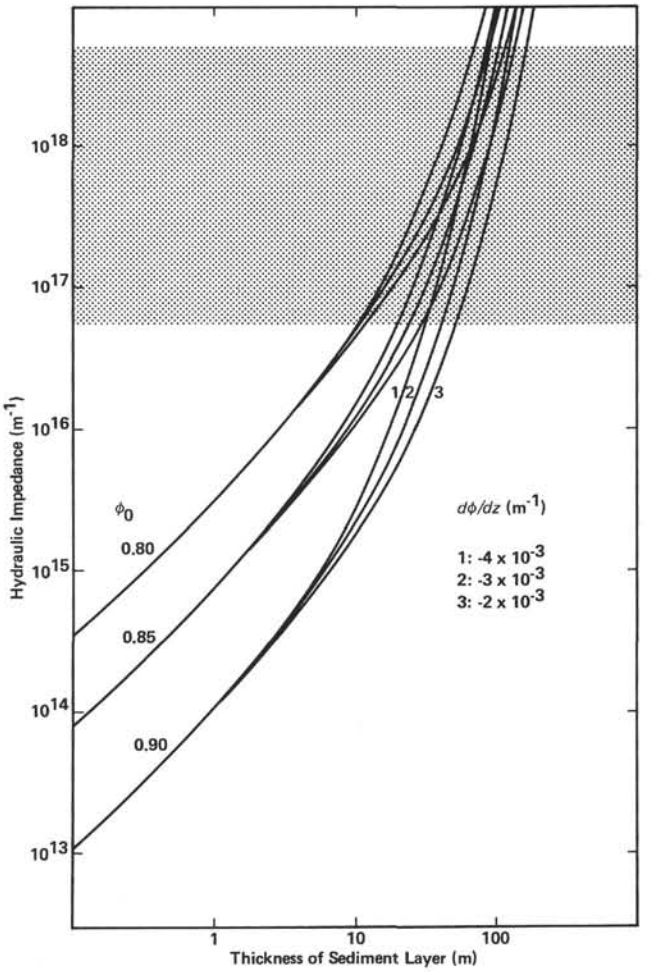

Figure 15. Hydraulic impedance versus sediment layer thickness relations calculated by the relation $I = \int_0^h dz/K_{sed}(Z)$, using permeability vs. porosity relation of Bryant et al. (1974) and assuming $\phi = \phi_0 + (d\phi/dz)z$. (Hydraulic impedance of sediment layer with about 50 m thickness is comparable to that of basement layer, if the thickness and average permeability of basement layer is about 2–3 km and 2–30 millidarcy, respectively.)

would then reflect the cessation of the highly effective hydrothermal dissolution processes. It would also imply that the sediment thickness at which this discontinuity occurs—about 50 meters—is a threshold thickness for sealing off generalized hydrothermal exchange through the sediment. This is consistent with the approach of measured heat flow to that predicted at a relatively young age at the Galapagos Spreading Center. It also allows us to make a reasonable estimate of the permeability of the underlying basaltic layer.

The linearity of the gradients and their correlation with surface heat flow suggest relatively constant local hydrothermal conditions through the early plate history of a sediment column. This agrees well with the numerical results of Green (1980). Thus our data suggest that some of the important hydrothermal conditions for the formation of mounds may have held constant for a relatively long time, so that long-term growth of mounds could occur. On the other hand, the same hydrothermal processes hasten the compaction of the sediments and increase their resistance to further hydrothermal circulation. Therefore, formation of mounds probably cannot

occur when the sediment cover exceeds about 50 meters in the Galapagos region.

ACKNOWLEDGMENTS

We wish to express our appreciation for the opportunity to participate on Leg 70 of DSDP. We thank Jim Pine for the gravimetric measurements, Dick Von Herzen for discussion, Naoyuki Fujii and Kei Kurita for reviewing the manuscript, and Sayuri Washida for typewriting the manuscript.

REFERENCES

Anderson, R. N., and Hobart, M. A., 1976. The relation between heat flow, sediment thickness, and age in the eastern Pacific. *J. Geophys. Res.*, 81:2968–2989.

Anderson, R. N., Langseth, M. G., and Sclater, J. G., 1977. The mechanisms of heat transfer through the floor of the Indian Ocean. *J. Geophys. Res.*, 82:3391–3409.

Boyce, R. E., 1976. Definitions and laboratory techniques of compressional sound velocity parameters and wet-water content, wet-bulk density, and porosity parameters by gravimetric and gamma ray attenuation techniques. *In* Schlanger, S. O., Jackson, E. D., et al., *Init. Repts. DSDP*, 33: Washington (U.S. Govt. Printing Office), 931–958.

_____, 1977. Deep Sea Drilling Project procedures for shear strength measurement of clayey sediment using modified Wykeham Farrance laboratory vane apparatus. *In* Baker, P. F., Dalziel, I. W. D., et al., *Init. Repts. DSDP*, 36: Washington (U.S. Govt. Printing Office), 1059–1068.

Bryant, W. R., Deflache, A. P., and Trabant, P. K., 1974. Consolidation of marine clays and carbonates. *In* Inderbitzen, A. L. (Ed.), *Deep Sea Sediments:* New York (Plenum Press), pp. 209–244.

Green, K. E, 1980. Geothermal Processes at the Galapagos Spreading Center [PhD dissert.]. Massachusetts Institution of Technology, Woods Hole Oceanographic Institution.

Green, K. E., Von Herzen, R. P., and Williams, D. L., 1981. The Galapagos. Spreading Center at 86°W: A detailed geothermal field study. *J. Geophys. Res.*, 86:979–986.

Hamilton, E. L., 1976. Variation of density and porosity with depth in deep-sea sediments. *J. Sed. Petrol.*, 46:280–300.

Lonsdale, P., 1977. Deep-tow observations at the mounds abyssal hydrothermal field, Galapagos Rift. *Earth Planet. Sci. Lett.*, 36: 92–110.

Mayer, L. A., 1979. The origin of fine scale acoustic stratigraphy in deep-sea carbonates. *J. Geophys. Res.*, 84:6177–6184.

Nafe, J. E., and Drake, C. L., 1957. Variation with depth in shallow and deep water marine sediments of porosity, density and the velocities of compressional and shear waves. *Geophysics*, 22:523.

Natland, J. H., Rosendahl, B. R., Hekinian, R., Briqueu, L., Dmitriev, Y., Fodor, R. V., Goll, R. M., Hoffert, M., Humphris, S. E., Mattey, D. P., Natland, J. H., Petersen, N., Roggenthen, W., Schrader, E. L., Srivastava, R. K., and Warren, N., 1979. Galapagos hydrothermal mounds: Stratigraphy and chemistry revealed by deep sea drilling. *Science*, 204:613–616.

Von Herzen, R. P., and Maxwell, A. E., 1959. The measurement of thermal conductivity of deep sea sediments by a needle-probe method. *J. Geophys. Res.*, 64:1557–1563.

Wilkens, R. H., and Langseth, M. G, in press. Physical properties of sediments from Sites 504 and 505. *In* Cann, J. R., Langseth, M. G., Honnorez, J., Von Herzen, R. P., White, S. M., et al., *Init. Repts. DSDP*, 69: Washington (U.S. Govt. Printing Office).

Williams, D. L., Von Herzen, R. P., Sclater, J. G., and Anderson, R. N., 1974. The Galapagos Spreading Centre: Lithospheric cooling and hydrothermal circulation. *Geophys. J. R. Astron. Soc.*, 38: 587–608.